Environmental Science & Technology

pubs.acs.org/est

Article

# Binding of Dissolved Organic Matter to RNA and Protection from Nuclease-Mediated Degradation

Anamika Chatterjee, Ke Zhang, and Kimberly M. Parker*

Cite This: *Environ. Sci. Technol.* 2023, 57, 16086−16096

Read Online

ACCESS | Metrics & More | Article Recommendations | Supporting Information



**ABSTRACT:** The persistence of RNA in environmental systems is an important parameter for emerging applications, including ecological surveys, wastewater-based epidemiology, and RNA interference biopesticides. RNA persistence is controlled by its rate of biodegradation, particularly by extracellular enzymes, although the specific factors determining this rate have not been characterized. Due to prior work suggesting that nucleic acids—specifically DNA—interact with dissolved organic matter (DOM), we hypothesized that DOM may bind RNA and impede its biodegradation in natural systems. We first adapted a technique previously used to assess RNA-protein binding to differentiate RNA that is bound at all sites by DOM from RNA that is unbound or partially bound by DOM. Results from this technique suggested that humic acids bound RNA more extensively than fulvic acids. At concentrations of 8−10 $mg_C/L$, humic acids were also found to be more effective than fulvic acids at suppressing enzymatic degradation of RNA. In surface water and soil extract containing DOM, RNA degradation was suppressed by 39−46% relative to pH-adjusted controls. Due to the ability of DOM to both bind and suppress the enzymatic degradation of RNA, RNA biodegradation may be slowed in environmental systems with high DOM concentrations, which may increase its persistence.

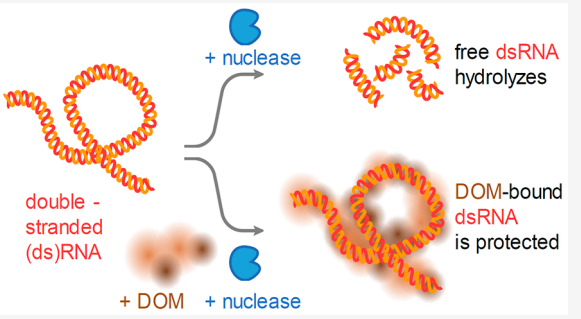


**KEYWORDS:** *single-stranded RNA, double-stranded RNA, dissolved organic matter, humic acid, fulvic acid, biological degradation, RNase I*

## INTRODUCTION

Nucleic acids (NAs, i.e., DNA and RNA) play a crucial role in supporting life and, as a result, are ubiquitous in the environment. Both NAs have been used in emerging technologies across environmental sciences. For example, environmental DNA has been analyzed to conduct ecological surveys[1−3] and to monitor the spread of antibiotic resistance genes.[4] Additional applications have been developed using RNA that leverage its unique attributes; in particular, its decreased persistence relative to DNA is often considered. For example, RNA is advantageous in ecological surveys because its lowered persistence facilitates the identification of metabolically active species at specific locations and times.[5,6] RNA abundances are also measured when monitoring RNA viruses using wastewater-based epidemiology;[7,8] relating the measured RNA abundances to initial viral loads requires consideration of RNA degradation rates.[9] Double-stranded (ds)RNA is also uniquely able to trigger a cellular process called RNA interference (RNAi),[10] which has been harnessed for pest control in agriculture.[11] The persistence of these dsRNA pesticides in environmental systems influences both their efficacy (particularly when applied exogenously[12,13]) as well as their potential risk to nontarget organisms arising from unintended exposure.[14,15] Due to its centrality across these applications, the persistence of RNA in environmental systems must be better constrained by improved understanding of key fate processes. While some of these processes likely parallel processes that impact DNA fate (e.g., adsorption to surfaces),[16] others (e.g., abiotic degradation or biodegradation) may diverge.[3,14,17]

One important process controlling both DNA and RNA persistence is biodegradation, which can in principle be mediated by both active microbes and extracellular enzymes in environmental systems (e.g., soil). The specific role of active microbes in DNA degradation has been supported by slower DNA loss in sterilized environmental media.[18−20] For example, while up to 77% of added DNA mass was degraded over 2 months in native soil microcosms, no degradation was detected when the soil was chemically sterilized.[19] In contrast, RNA degradation was unaffected,[21,22] only partially reduced,[21,23] or, in one case, increased[21] upon sterilization of environmental

Received: June 27, 2023
Revised: September 11, 2023
Accepted: September 19, 2023
Published: October 9, 2023

media spanning soils, wastewater, and surface water. RNA degradation in sterilized media is unlikely to be attributable to known abiotic pathways,[24−26] which are typically too slow to account for the observed rapid loss of RNA,[25,26] Instead, enzymes (i.e., RNases), which are incompletely inactivated by sterilization,[27,28] may continue to degrade RNA, indicating that nuclease enzymes may play a greater role in limiting the persistence of RNA than DNA in the environment.

While biodegradation is expected to drive NA loss, these processes may be slowed in the presence of environmental constituents such as minerals and organic matter (OM). The adsorption of DNA to clay minerals and other particles is well-established to protect DNA from biodegradation.[29−36] Similarly, certain clays have been shown to slow biodegradation of RNA after its adsorption.[37,38] Beyond adsorption to mineral surfaces, some studies found that DNA adsorption to OM-coated surfaces also impedes its enzymatic degradation.[32,39,40] For example, when subjected to DNase-mediated degradation, the remaining copy numbers of DNA adsorbed to humic acid (HA)-coated nanoparticles were orders-of-magnitude higher compared to free DNA.[40] The protection of NAs have been attributed to their reduced accessibility to nucleases upon adsorption to HA-coated nanoparticles,[40] as also proposed for other surfaces.[31,32,36,41] The adsorption of nucleases themselves has also been proposed as an additional factor that may reduce NA degradation.[29,35,40]

Although the adsorption of DNA and, to a lesser extent, RNA to surfaces has been previously examined, knowledge regarding the binding of dissolved organic matter (DOM) to NAs and its potential to increase their persistence remains limited. To date, studies on NA-OM interactions have primarily investigated cases where one component (typically the OM,[32,39,42−46] though in one case DNA[47]) is adsorbed to a solid support to facilitate separation of the adsorbed material from solution. These studies have identified the roles of electrostatic charge screening and cation bridging[32,39,44−47] in driving NA adsorption to OM, in addition to proposing contributions from hydrogen bonding, the hydrophobic effect, and van der Waals interactions.[42,43] Binding of soil-extracted HAs to DNA in solution, which may slow DNA biodegradation,[48] has been characterized.[48,49] However, these studies separated DNA bound to HAs from free DNA using centrifugation,[48,49] which may underestimate binding if bound DNA remains dissolved. Instead, we hypothesized that binding of DOM to NAs might alternatively be characterized by adapting techniques that have been previously applied to explore binding between NAs and other dissolved molecules like proteins.[50−52]

In this study, we evaluated the ability of DOM to bind to RNA and protect it from nuclease-mediated degradation. To characterize RNA-DOM binding, we adapted the electrophoretic mobility shift assay (EMSA), which is conventionally applied to assess binding of macromolecules (e.g., proteins) to NAs using separation based on size and charge.[50−52] While we determined that the technique could be applied to evaluate RNA-DOM binding, we also identified key differences in how the technique functions in this context relative to its conventional application, supported by our use of homopeptides as DOM surrogates with known structures and chemistries. Using the adapted approach, we compared RNA-DOM binding as a function of RNA and DOM characteristics (e.g., RNA length and structure and DOM type). After identifying the factors that influence RNA-DOM binding, we then tested their correlation to the ability of DOM to suppress the enzymatic degradation of RNA in solution. Expanding upon these results collected using DOM isolates, we evaluated the ability of DOM occurring in authentic soil and river water samples to also protect RNA from degradation to validate the impact of DOM on the environmental persistence of RNA.

## MATERIALS AND METHODS

**Material Sources, Preparation, and Characterization.** The sources of materials and supplies are detailed in Section S1. RNA molecules (i.e., single-stranded (ss)RNA, 1006 nucleotides (nt); dsRNA, 100 and 1000 base pairs (bp), spanning the sizes of dsRNA biopesticides[37,53,54]) were synthesized following an established protocol[25] (sequences in Section S2). Modeling of the secondary structure of the ssRNA molecule indicated extensive folding (Figure S1).[55] Concentrations of the prepared stock solutions were measured using ultraviolet (UV) light absorbance via a NanoDrop One$^c$ spectrophotometer (extinction coefficients of 0.0214 and 0.0266 $(mg/L)^{-1}$ $cm^{-1}$ for dsRNA and ssRNA, respectively).[56] RNA size after synthesis was confirmed by gel electrophoresis. RNase I enzyme (10 U/$\mu$L) was provided by the manufacturer in a mixture containing 50 mM tris(hydroxymethyl)-aminomethane-hydrochloride (Tris-HCl, pH 8), 100 mM sodium chloride (NaCl), 0.01% Triton-X, and 50% (v/v) glycerol.[57] The final concentrations of these constituents in RNase-containing samples are reported in the corresponding figure captions. The RNase I mixture was stored at −20 °C in an enzyme-rated freezer (ThermoFisher) until use.

DOM isolates used in this study include Pahokee peat HA (PPHA, 1S03H), Leonardite HA (LHA, 1S04H), Suwanee River fulvic acid II (SRFA, 2S101F), Suwanee River natural organic matter II (SRNOM, 2R101N), and Elliott Soil fulvic acid V (ESFA, 5S102F), which were selected to span the range of reported polarities and charge densities among available International Humic Substances Society (IHSS) isolates (Table S2).[58−60] We prepared DOM stock solutions by adding individual IHSS isolates to ultrapure water (>18.2 MΩ cm) and adjusting pH to 7 using 1 M hydrochloric acid or sodium hydroxide. After being mixed overnight, the prepared stocks were filtered using sterile syringes and 0.22 $\mu$m polyvinylidene difluoride filters. Their organic carbon concentrations were measured in duplicate (replicate error < 10%) using a total organic carbon analyzer (Shimadzu TOC-L) (Table S3).

We also collected a soil extract and a surface water sample that contained DOM. The soil extract was collected as the supernatant of a suspension prepared by adding buffer to a characterized silty clay loam soil (Table S4)[61] as described in Section S3.1.[62,63] The surface water sample was collected from the Missouri River near St. Charles, Missouri, and filtered with a 0.22 $\mu$m poly(ether sulfone) membrane. Characterized soil extract and river water quality parameters are reported in Table S4 and Table S5, respectively. The soil extract and river water were stored at 4 °C until use.

We followed a previously established protocol to prevent RNA degradation due to inadvertent contamination of samples by RNases or microbes.[25,26] Specifically, plastic supplies were either purchased as certified RNase-free or treated with 0.1% diethylpyrocarbonate. Glassware was baked at 450 °C for 4 h, and aqueous stock solutions (e.g., buffers) were autoclaved before use. An exception was made for the DOM stocks, which


https://doi.org/10.1021/acs.est.3c05019
Environ. Sci. Technol. 2023, 57, 16086−16096

were filter-sterilized but not autoclaved to avoid modifications to the DOM chemical properties. In the binding experiments, lower molecular weight products were not detected via gel electrophoresis, ruling out unintended degradation.[17,23] Additionally, because DOM had an inhibitory effect on RNase I-mediated RNA degradation, as determined in the degradation experiments detailed below, the contribution of residual RNases in DOM solutions to RNA degradation was inferred to be negligible relative to RNase I added as a reagent.

**RNA-DOM and RNA-Homopeptide Binding Experiments.** Binding experiments were performed in 2 mL Protein LoBind tubes, which have been found to negligibly sorb RNA to the tube walls.[23] The RNA concentrations were confirmed using UV absorbance immediately before addition to incubation mixtures, which were prepared by combining 3-(*N*-morpholino)-propanesulfonic acid (MOPS) buffer, NaCl, RNA, and DOM in a total solution volume of 20 $\mu$L (corresponding to the volume loaded into gels). In some experiments, DOM was replaced with the homopeptides poly-L-lysine (PLL) and poly-L-threonine (PLT), which served as DOM surrogates to determine how site-independent binding to dsRNA affected its analysis by gel electrophoresis. The two homopeptides are polymers with well-defined structures and established charges, and their size ranges (Table S6) are comparable to DOM (Table S2).[52,64−66] All samples contained 25 mg/L RNA, 3 mM MOPS, and 10 mM NaCl as well as PLL, PLT, or DOM at concentrations specified in the corresponding figure captions and were incubated over 0.6−1 h. At these conditions, DOM primarily remained dissolved, as indicated by no change in solution absorbance after centrifugation (14,800 rpm, 0.5 h, Figure S2). In the case of RNA-DOM binding, no change in binding over a period of 5 min−12 h was observed (Figure S3), indicating that incubation times used were sufficient to achieve equilibrium.

To quantify RNA concentrations after incubation, samples were loaded using 6X Orange DNA Gel Loading Dye into gels following a previously described gel electrophoresis technique.[26] Briefly, gels were made of 1.5% [w/w] agarose in Tris-acetate-ethylenediaminetetraacetic acid (TAE) buffer (pH 8.4 ± 0.1)[67] and 0.01% [v/v] SYBR Safe stain. Gels were run at 150 V for 30 min.

Gels were imaged on a gel imaging system (VisionWorksLS), and the RNA signal was quantified using ImageJ (version 1.53a), according to the protocol described in Section S5.2.[25] The binding data were fit by the Hill equation (eq 1),[68] which was adapted from its conventional use for modeling RNA-protein binding measured by EMSA.[50,51] Unlike EMSA, where the parameter $Y$ represents the fraction of bound RNA, we instead represented $Y$ as RNA signal loss, as detailed below in the subsection Application of Gel Electrophoresis to Assess Binding of DOM to RNA in the Results and Discussion.

$$Y = \frac{B_{max} \times X^h}{K_D^h + X^h} \quad (1)$$

The Hill parameters $B_{max}$, $X$, $K_D$, and $h$ represent the maximum calculated RNA signal loss, the applied PLL or DOM concentration, the PLL or DOM concentration at $Y$ = 0.5, and the Hill slope, respectively. The Hill slope is typically 1 for RNA-protein binding. Deviations in the value of Hill slope from 1 (either $h > 1$ or $h < 1$) are representative of scenarios where multiple proteins bind to RNA.[50]

**RNase I-Mediated RNA Degradation Experiments.** The inhibitory effect of DOM on RNase I-mediated degradation was primarily evaluated by comparing the production of monomeric hydrolysis products (i.e., 3′-nucleoside monophosphates, 3′-NMPs) in RNA samples incubated either in the presence or absence of DOM. RNase I, a member of the RNase T2 family[57,69] found broadly across diverse organisms,[69,70] was selected for its ability to hydrolyze RNA phosphodiester bonds to 3′-NMPs without the addition of cofactors.[71] Incubation mixtures were prepared by combining the MOPS buffer, NaCl, and RNA, ensuring that their final concentrations matched RNA-DOM binding experiments. DOM (at concentration of 8−10 and 61−69 $mg_C/L$) was added to a subset of samples. All samples had a total volume of 79.0−79.5 $\mu$L. The solutions were vortexed and then briefly centrifuged to spin down any liquid droplets and incubated without shaking for 2.0−2.6 h at ambient laboratory temperature, which were measured using a Durac Plus thermometer (ThermoFisher) and reported in the corresponding figure captions. After RNA-DOM incubation, we applied RNase I at 5 U (for ssRNA) or 10 U (for dsRNA, which RNase I is less active toward[72]) to generate sufficient amounts of 3′-NMPs over the duration of the degradation experiments (up to 9 h).

To determine the extent of RNase I-mediated RNA degradation, concentrations of a specific 3′-NMP, namely 3′-adenosine monophosphate (3′-AMP), were quantified using high pressure liquid chromatography (HPLC) with UV detection (Section S6).[25] Slight variations in 3′-AMP generation were observed across DOM-free control samples during different experiments, ranging from 7.2(±0.1)−9.1(±0.6) $\mu$M at 8.1−8.3 h (Figure 3). Consequently, to account for the variations in 3′-AMP generation, we assessed the inhibition of RNA degradation by DOM relative to the DOM-free control within the same experiment.

The amount of 3′-AMP generated was similarly used to assess RNase I-mediated dsRNA degradation in soil extract and river water with a few modifications. Specifically, these experiments comprised a pH-matched buffer control containing 10 U RNase I. Additionally, soil extract and river water were incubated with dsRNA either in the absence or presence of 10 U RNase I. The river water experiment was conducted over a longer duration of 16.7 h compared to 7−9 h because the river water had a higher pH (8.04 ± 0.04) compared to other experiments performed at pH 7, which may reduce enzymatic activity,[73] as evidenced by the lowered 3′-AMP generation in the pH-matched buffer control (Figure 4B).

The suppression of RNA degradation by PPHA was also analyzed using the quantitative reverse transcription polymerase chain reaction (RT-qPCR). PPHA was added to a subset of the buffer-dsRNA mixtures immediately before the addition of RNase I up to a total volume of 100 $\mu$L. The final concentrations of all constituents are reported in the corresponding figure caption. Following an incubation of 1 h, all samples were serially diluted 100-fold before analysis by RT-qPCR. This dilution factor was selected to prevent inhibition by PPHA (Section S7).[26]

**Statistical Analysis.** All experiments were performed using duplicate samples prepared separately. Error bars represent the range of the sample values. The 90% confidence intervals ($CI^{90\%}$) for Hill parameters were calculated using GraphPad Prism 9.0. Differences in Hill parameters were evaluated for statistical significance using the extra-sum-of-squares F test.


https://doi.org/10.1021/acs.est.3c05019
Environ. Sci. Technol. 2023, 57, 16086−16096

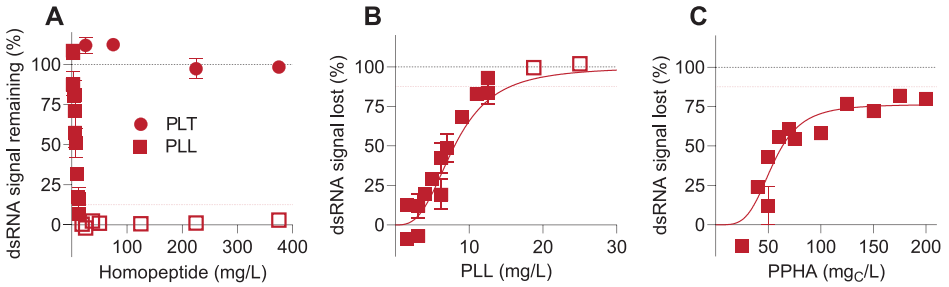


**Figure 1.** Binding of homopeptides and PPHA to 1000 bp dsRNA at 24−25 °C. Experiments were conducted at pH 7 (3 mM MOPS, 10 mM NaCl). All samples contained dsRNA at an expected initial concentration of 25 mg/L. (**A**) The signal remaining of dsRNA was measured after incubation with homopeptides PLL and PLT at specified concentrations for 1 h. The red dashed line represents the lower limit of measurable signal remaining (12.5%). The data points below the measurable lower limit are represented with open squares. (**B**−**C**) The signal loss of dsRNA was measured after incubation with PLL or PPHA at specified concentrations for 1 h or 0.6−0.7 h, respectively. Individual replicates were fitted with the Hill equation (eq 1, $B_{max}$ constrained to values ≤ 100%). The red dashed line represents the upper limit of measurable signal loss (87.5%). The PLL data points above the measurable upper limit are represented with open squares and were not included in the Hill equation fit. Error bars represent the range of two replicate experiments; error bars not visible are smaller than the symbols.

Differences in hydrolysis product concentrations were evaluated for statistical significance using an unpaired Student's *t*-test. For both statistical significance tests, the confidence level was set as $p \leq 0.05$.

## RESULTS AND DISCUSSION

**1. Application of Gel Electrophoresis to Assess Binding of DOM to RNA.** To assess whether DOM binds RNA, we adapted EMSA, a technique that uses separation by gel electrophoresis to assess binding of biomacromolecules (e.g., proteins) to NAs.[50−52] Typically, proteins bind to RNA (e.g., ssRNA) at specific sites, while the rest of the RNA molecule does not interact.[50] Due to the difference in their relative size and charge, the free and the protein-bound RNA appear as two separate bands in the gel.[50,51] In contrast, we hypothesized that DOM would bind RNA at multiple sites as a result of interactions between their functional groups located throughout their structure,[43] which we referred to as site-independent binding. Consequently, we first aimed to evaluate how this difference in binding type would affect the detection of DOM-bound RNA when using gel electrophoresis.

In initial tests, we used the selected homopeptides as surrogates for DOM. We expected PLL, which is cationic at circumneutral pH,[64] to strongly bind negatively charged dsRNA (isoelectric point ∼5−7)[74] by electrostatic interactions. PLL has previously been found to bind DNA[52] as well as dsRNA[75] (though notably aggregates were removed before analysis using a 50 kDa filter, differing from our procedure). In contrast to PLL, PLT is neutral at circumneutral pH[64] and therefore not expected to bind RNA strongly. In agreement with our expectation, the addition of PLT had no effect on the migration of dsRNA in the gel (Figure S5). In contrast, PLL at the same concentration range resulted in decreasing intensity of the dsRNA band as well as a slight shift toward the anode (Figures S6, 1A), consistent with an aggregate with less overall negative charge relative to its size.[75]

In addition to decreasing the intensity of the free RNA band, increasing protein concentrations during EMSA leads to increasing intensity of a band corresponding to the protein-bound RNA.[50,51] In contrast, PLL-bound RNA was not visualized in the gel (Figure S6A), leading us to investigate possible causes. To ensure that dsRNA bound by PLL enters into the gel, we confirmed that residual dsRNA was not observed within the gel well (Figure S6) and that PLL-bound dsRNA was not lost to the gel running buffer (Section S8.2). Instead, our additional tests suggested that binding of PLL to dsRNA likely prevents fluorescent dye from intercalating into dsRNA bound by PLL at all available sites (Section S8.3). Partial suppression of dye intercalation may also occur for dsRNA partially bound by PLL, which may also not occur at sufficient levels to be visualized due to the polydispersity of PLL[52] resulting in aggregates with diverse sizes, charge states, and conformations that migrate to different distances in the gel. Our findings were consistent with DNA-PLL binding, wherein bound aggregates were not observed.[52] In contrast to PLL, proteins bind to a target sequence within the RNA molecule, resulting in the formation of a complex with a specific size, charge, and conformation,[50] thereby generating a distinct band in the gel as most of the RNA molecule remains available for dye intercalation. Due to these key differences from EMSA, we refer to our assay as gel electrophoresis throughout our study.

To evaluate the extent of RNA sites bound by PLL, we compared the relative amount of PLL required to result in significant dsRNA signal loss to the theoretical amount of PLL expected to bind to dsRNA (Section S8.4). Experimentally, dsRNA signal loss approached the upper limit of its measurable value (i.e., corresponding to lower limit of dsRNA signal remaining) when PLL was added at a concentration of 12.5 mg/L (Figures 1A, 1B), which corresponds to a mass ratio of PLL to dsRNA of 0.5 $mg_{PLL}$ per 1 $mg_{dsRNA}$. Theoretically, if each positively charged monomer in PLL bound one negatively charged nucleotide in dsRNA, we estimated that 0.4 $mg_{PLL}$ would be required to bind 1 $mg_{dsRNA}$. The similarity between these ratios suggests that signal loss occurs when sufficient PLL is present to bind to most available sites along the dsRNA molecule, consistent with extensive site-independent binding by PLL that prevents the intercalation of the fluorescent dye into dsRNA.

Due to the differences that we observed between dsRNA-PLL binding examined in our study relative to previously characterized RNA-protein binding,[50,51] we opted to report our data in terms of signal loss rather than the fraction of bound RNA, which is typically reported from EMSA.[50,51] The fraction of bound RNA is conventionally calculated using the intensities of the bands corresponding to the unbound and protein-bound RNA by assuming the fluorescent signal intensities of these bands are proportional to the RNA mass


https://doi.org/10.1021/acs.est.3c05019
Environ. Sci. Technol. 2023, 57, 16086−16096

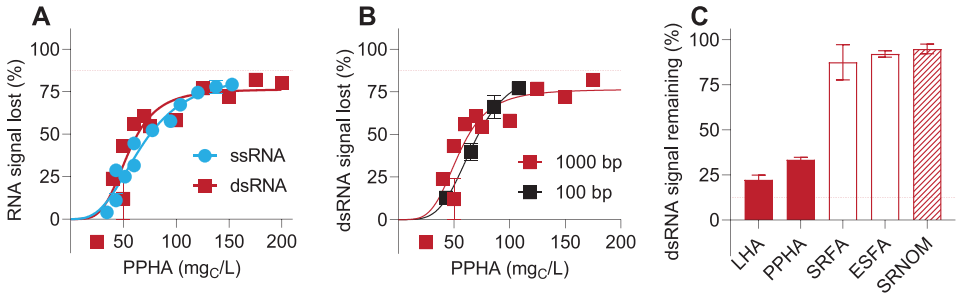


**Figure 2.** Binding between RNA and DOM characterized by gel electrophoresis. Experiments were conducted at pH 7 (3 mM MOPS, 10 mM NaCl) for 0.6−0.7 h at 23−26 °C. All samples contained RNA at an expected initial concentration of 25 mg/L. (**A**−**B**) The signal loss of RNA (1006 nt ssRNA and 1000 bp dsRNA, **A**; 100 and 1000 bp dsRNA, **B**) was measured after incubation with PPHA at specified concentrations. Individual replicates were fitted with the Hill equation (eq 1). The red dashed line represents the upper limit of measurable signal loss (87.5%). (**C**) DOM isolates LHA, PPHA, SRNOM, SRFA, and ESFA at a concentration of 70 $mg_C$/L were incubated with 1000 bp dsRNA. The red dashed line represents the lower limit of measurable signal remaining (12.5%). Error bars represent the range of two replicate experiments; error bars not visible are smaller than the symbols.

concentration.[50] In contrast, our results suggest that complete signal suppression is observed only when dsRNA is bound at all sites by PLL. Consequently, our approach can be used to differentiate between bound and unbound RNA but not to determine the fraction of RNA molecules bound by one or more PLL molecules. Despite these differences from EMSA, we found that signal loss from dsRNA-PLL binding could be fit to the Hill equation (eq 1, Figure 1B, $R^2$ = 0.88), revealing a Hill slope of 2.9 ($CI^{90\%}$ = 2.2−8.0), which indicated that multiple PLL molecules bound to dsRNA.

Using the framework developed to evaluate dsRNA-homopeptide binding, we next applied gel electrophoresis to evaluate dsRNA-DOM binding using PPHA. Unlike PLL, which can neutralize dsRNA via binding,[75] PPHA is unable to neutralize dsRNA due to its negative charge,[58] leading to the unaltered migration of the dsRNA band in the presence of PPHA (Figure S7). However, increasing PPHA concentrations resulted in decreasing dsRNA signal (Figure S8). Since PPHA, unlike PLL, is chromophoric, we considered the possibility that elevated PPHA concentrations could result in reduced dsRNA signal due to reduced dye fluorescence because of light screening by DOM, rather than reduced dye intercalation into bound RNA. To test this, we incubated different initial concentrations of dsRNA with a fixed concentration of PPHA and measured subsequent signal losses. If light screening by DOM was causing decreased dsRNA signal, we would observe that dsRNA signal losses were lowered by a consistent percentage. However, we observed that the percentage of the signal loss was higher at lower dsRNA concentrations (Figure S9), which was indicative of dsRNA-PPHA binding being the dominant cause of reduced dsRNA signal rather than light screening. Similar to dsRNA-PLL binding, we anticipate that partial binding of dsRNA by PPHA may result in the generation of aggregates of diverse sizes and charges that occur at individually low concentrations and be subject to suppression of dye intercalation into dsRNA, such that they remained undetectable by gel electrophoresis.

The dsRNA-PPHA binding data were also fit by the Hill equation (Figure 1C, $R^2$ = 0.85). The fit revealed a Hill slope of 4.1 ($CI^{90\%}$ = 2.5−6.9), which indicated that multiple DOM molecules bound to dsRNA, similar to dsRNA-PLL binding. However, there were notable differences between dsRNA-PLL and dsRNA-PPHA binding. The $K_D$ for dsRNA-PPHA binding was 12-fold higher on a per carbon basis (54.3 $mg_C$/L, $CI^{90\%}$ = 48.5−63.1 $mg_C$/L) compared to dsRNA-PLL binding, which had a $K_D$ of 4.5 $mg_C$/L ($CI^{90\%}$ = 3.2−4.7 $mg_C$/L). This result indicated that, at the same dsRNA concentration, PPHA was required to be at a higher concentration relative to PLL to result in 50% dsRNA signal loss. Furthermore, the $B_{max}$ for dsRNA-PPHA binding was 77% ($CI^{90\%}$ = 69−88%), in contrast to dsRNA-PLL binding that reduced signal beyond measurable limits. The lower $B_{max}$ for dsRNA-PPHA binding indicated that binding of dsRNA by PPHA did not lead to complete suppression of fluorescent dye intercalation, unlike dsRNA-PLL binding.

**2. Assessment of Factors Controlling RNA-DOM Binding.** After demonstrating that DOM binds to dsRNA, we next aimed to elucidate the key factors that may control their binding as a result of driving forces. Binding between DNA and OM is governed by a combination of driving forces including charge screening, cation bridging, reduced electrostatic repulsion, hydrogen bonding, and van der Waals force.[43−45] To explore the contribution of these driving forces to RNA-DOM binding, we systematically tested the effect of parameters including solution chemistry, RNA type (i.e., ssRNA or dsRNA) and length, and DOM type, polarity, and charge densities on RNA-DOM binding.

We first examined the effect of solution chemistry on dsRNA-DOM binding. This approach is commonly employed to determine the contribution of charge screening, cation bridging, and reduced electrostatic repulsion in driving binding of biomacromolecules to OM-coated surfaces.[44,45,58] However, we anticipated that gel electrophoresis might not be able to assess the effect of solution chemistry, because the chemistry of the gel running buffer may determine binding instead of the incubation buffer. Studies using EMSA have typically applied gel running buffers with fixed solution chemistries and do not adjust the solution during incubation.[50,51] We varied the solution chemistry of our incubation buffer by modulating the ionic strength through the applied NaCl concentration or by introducing orthophosphate as a binding competitor (Section S8.6). These changes were made only during the incubation period, while the gel running conditions remained constant. As expected, the resultant dsRNA signal loss was unaffected by the changes in solution chemistry, indicating that gel electrophoresis was ultimately dependent on the composition of the gel running buffer (40 mM Tris, 20 mM acetic acid, 1 mM EDTA, pH 8.4 ± 0.1).[67]

To investigate the impact of RNA type on RNA-PPHA binding, we compared the binding of 1000 bp dsRNA and


https://doi.org/10.1021/acs.est.3c05019
Environ. Sci. Technol. 2023, 57, 16086−16096

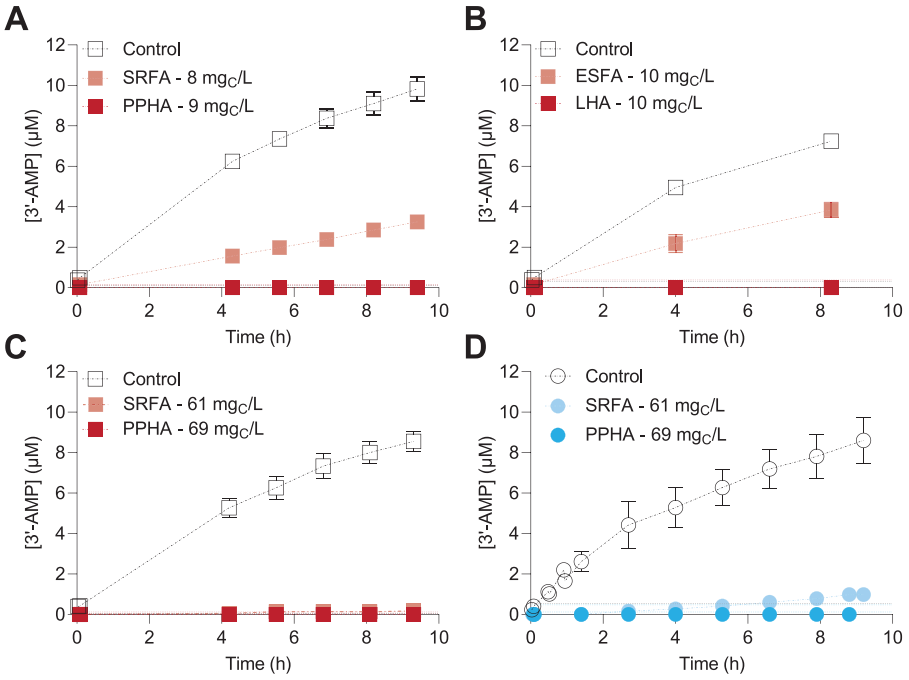


**Figure 3.** RNase I-mediated degradation of RNA in the presence of DOM isolates. Experiments were conducted at pH 7 (3 mM MOPS, 10 mM NaCl) at 23−26 °C. All samples contained either 1000 bp dsRNA (**A-C**) or 1006 nt ssRNA (**D**) at an expected initial concentration of 25 mg/L with DOM isolates added as indicated in the figure legends. The suppression of RNA degradation by DOM was assessed relative to the DOM-free control within the same experiment. In dsRNA-containing samples (**A-C**), RNase I was added at an activity of 10 U; therefore, the samples also contained 0.6 mM Tris-HCl, 1.3 mM NaCl, 0.0001% Triton-X, and 0.6% (v/v) glycerol that were present in the RNase I mixture. In the ssRNA-containing samples (**D**), RNase I was added at an activity of 5 U, resulting in correspondingly lower concentrations of constituents in the enzyme mixture. Error bars represent the range of two replicate experiments; error bars not visible are smaller than the symbols. The dashed lines indicate the limits of detection.

1006 nt ssRNA. Previously, HA-coated nanoparticles had demonstrated similar adsorption to both ssDNA and dsDNA at the higher DNA concentrations tested.[43] However, at the lower DNA concentrations, the adsorption of HA-coated nanoparticles to ssDNA was slightly higher relative to dsDNA. This was attributed to the exposed bases of ssDNA, which were proposed to lower electrostatic repulsion and increase the likelihood of forming hydrogen bonds with HA.[43] In contrast, we found that the Hill parameters for ssRNA and dsRNA binding by PPHA were not statistically significantly different ($p$ = 0.18, Figure 2A), consistent with the extensive folding in the ssRNA structure (Figure S1).[55]

We next investigated the impact of RNA length on its binding by DOM by comparing the binding of PPHA to 100 and 1000 bp dsRNA. For adsorption of HA-coated nanoparticles to DNA, it was observed that the 508 bp DNA fragment exhibited modestly higher adsorption compared with the longer 680 and 861 bp fragments.[43] This difference was attributed to size exclusion or diffusion limitation effects that impeded the longer DNA fragments from accessing pores within the OM-coated surface.[43] However, for dsRNA-DOM binding, we hypothesized that the dsRNA length would not influence binding due to the availability of equivalent numbers of total binding sites in both 100 and 1000 bp dsRNA at the same mass concentration. We observed that our result aligned with our hypothesis because the calculated Hill parameters for the two dsRNA lengths were not statistically significantly different ($p$ = 0.41, Figure 2B). Thus, our result confirmed that binding by DOM was independent of the dsRNA length.

The binding of other selected DOM isolates to 1000 bp dsRNA was then assessed in order to examine the effect of the DOM type on binding. At a concentration of 70 $mg_C$/L, at which PPHA had previously demonstrated binding to dsRNA (Figure 2B), we observed that LHA also bound to dsRNA, as evidenced by the dsRNA remaining signals of 22(±3)−33(±1)% (Figure 2C). In contrast, both SRFA and ESFA had higher dsRNA remaining signals, exceeding 88%, implying that FAs had lower binding to dsRNA relative to HAs. Extensive binding of SRFA to RNA was not observed even across a wide range of SRFA concentrations (8−120 $mg_C$/L, Figure S12), indicating that SRFA binding to dsRNA was lower than the HAs even at higher SRFA concentrations. Similar to the FAs, SRNOM demonstrated a dsRNA remaining signal of 94.9(±2.7)%, indicating that SRNOM also had lower binding to dsRNA relative to HAs. Overall, this result indicates that HAs bind dsRNA to greater extents relative to other DOM types.

By analyzing the correlation between dsRNA signal loss and specific DOM properties (Table S2), we evaluated the potential contributions of various driving forces to dsRNA-DOM binding. We began by correlating dsRNA signal loss to DOM polarity, which was represented as the molar ratio of combined oxygen, nitrogen, and sulfur to carbon.[58] We found that the dsRNA signal loss decreased with increasing DOM polarity (Figure S13A), indicating the potential contribution of the hydrophobic effect to drive RNA-DOM binding, as observed for binding of other polyelectrolytes (i.e., proteins) to OM-coated surfaces.[58] We also correlated dsRNA signal loss to the carboxyl charge density of DOM and observed that signal loss increased as the carboxyl charge density decreased (Figure S13B), suggesting that lower electrostatic repulsion between RNA and DOM also contributes to binding. In


https://doi.org/10.1021/acs.est.3c05019
Environ. Sci. Technol. 2023, 57, 16086−16096

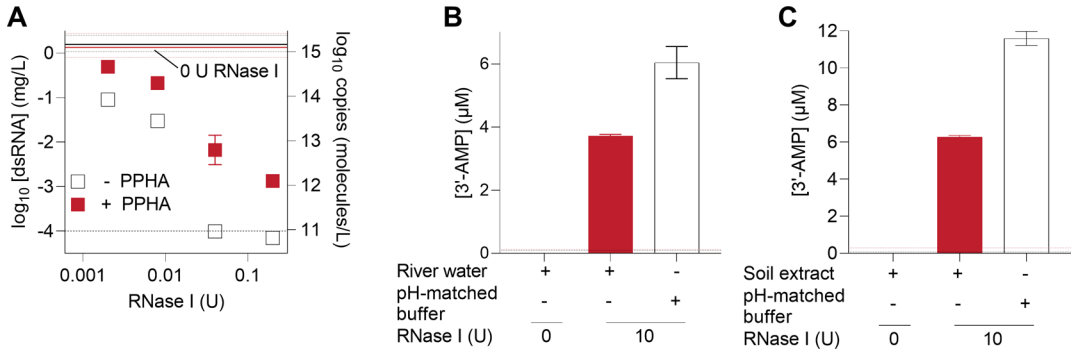


**Figure 4.** RNase I-mediated degradation of 1000 bp dsRNA in the presence of DOM at 23−26 °C. (**A**) Loss of intact dsRNA (added at 1 mg/L) measured by RT-qPCR incubated with PPHA (0 or 9 $mg_C$/L) and RNase I (0.002−0.2 U) at pH 7 (3 mM MOPS, 10 mM NaCl) in a total volume of 100 $\mu$L over 1 h. Labeled lines indicate samples with 0 U RNase I without (black) and with (red) PPHA; solid and dashes lines indicate means and ranges, respectively. (**B**−**C**) The generation of 3′-AMP was measured in surface water and soil extract containing DOM by HPLC-UV. All samples contained dsRNA at an expected initial concentration of 25 mg/L and RNase I (0 or 10 U). The reaction was monitored in either the Missouri River water (2.4 $mg_C$/L) or the buffer control (3 mM MOPS, 10 mM NaCl) over 16.7 h (**B**) and in either the soil extract (11.4 ± 0.2 $mg_C$/L) or the buffer control, both containing 6 mM MOPS and 20 mM NaCl over 7 h (**C**). RNase I was added at an activity of 10 U (**B**−**C**); therefore, the samples also contained 0.6 mM Tris-HCl, 1.3 mM NaCl, 0.0001% Triton-X, and 0.6% (v/v) glycerol that were present in the RNase I mixture. In panel (**A**), RNase I was added at an activity of 0.002−0.2 U, resulting in correspondingly lower concentrations of constituents in the enzyme mixture. The dashed lines indicate the lowest quantifiable standard (**A**) or the limits of detection (**B**−**C**). Error bars represent the range of two replicate experiments; error bars not visible are smaller than the symbols.

contrast, we found that the signal loss was not correlated to the phenolic charge density of the DOM (Figure S13C). While we tested the effect of polarity and charge density, correlated DOM properties (i.e., aromaticity, molecular weight) might also play a role in influencing dsRNA-DOM binding.

**3. Effect of DOM on RNase I-Mediated RNA Degradation.** Following our finding that the DOM type determines binding to RNA, we examined whether the DOM type was also related to the ability of DOM to protect RNA from enzymatic degradation. We first compared the capacity of PPHA and SRFA at 8−9 $mg_C$/L to protect dsRNA from enzymatic degradation at pH 7, by monitoring the production of 3′-AMP. We found that PPHA completely inhibited dsRNA degradation relative to the DOM-free control (Figure 3A). In addition, SRFA also suppressed degradation, albeit by a lower extent of 66.82(±0.02)% relative to the control at 9.4 h, indicating that PPHA was more effective than SRFA at protecting dsRNA from degradation. The difference in dsRNA protection between PPHA and SRFA can be attributed to the higher capacity of PPHA to bind dsRNA relative to that of SRFA (Figure 2C). This correspondence indicated that binding of dsRNA by DOM lowered its accessibility to RNase I, thereby reducing dsRNA degradation. An additional factor may be the higher encapsulation of enzymes by PPHA relative to SRFA, which may lower enzymatic activity,[60] and further contribute to the observed differences in dsRNA protection by different DOM types.

To further explore the generalizability of our findings with PPHA and SRFA, we extended our investigation to other DOM isolates, LHA and ESFA. We found that at 10 $mg_C$/L, LHA completely suppressed dsRNA degradation at 8.3 h (Figure 3B), similar to PPHA (Figure 3A). In contrast to LHA, 10 $mg_C$/L ESFA suppressed degradation to a lower extent of 46.8(± 0.1)% relative to the control at 8.3 h. Consequently, at DOM concentrations of 8−10 $mg_C$/L, which are within the upper bound of DOM concentrations reported in surface waters,[76−78] HAs demonstrated an enhanced capacity to protect dsRNA from degradation relative to FAs.

To examine whether higher concentrations of FAs resulted in greater suppression of dsRNA degradation relative to their lower concentrations, we next investigated degradation in the presence of SRFA at 61 $mg_C$/L in comparison to PPHA at 69 $mg_C$/L. We found that PPHA completely inhibited degradation at the higher concentration (Figure 3C), consistent with the complete suppression of degradation observed at the lower concentration (Figure 3A). Meanwhile, SRFA at 61 $mg_C$/L inhibited 3′-AMP production by 97.934(±0.002)% relative to the control at 9.3 h, marginally lower than the inhibition observed with PPHA (Figure 3C). Our result demonstrated that high DOM concentrations resulted in complete inhibition of enzymatic degradation of dsRNA.

In addition to the DOM type, we examined the effect of the RNA type on the ability of DOM to protect RNA from enzymatic degradation. Since RNase I is selective for ssRNA,[71] we applied lower enzymatic activity for 3′-AMP generation. Relative to the control, PPHA at 69 $mg_C$/L completely inhibited 3′-AMP production (Figure 3D), similar to the result observed with dsRNA degradation (Figure 3C). SRFA also suppressed ssRNA degradation relative to the control, as demonstrated by an 88.54(±0.01)% reduction in 3′-AMP concentration at 9.2 h (Figure 3D). According to our results, DOM was effective in protecting both RNA types.

While the formation of 3′-AMP is specific to enzymatic hydrolysis of RNA,[79] loss of detectable RNA measured by RT-qPCR can occur due to many different processes. However, because RT-qPCR is widely used to measure RNA in environmental applications,[7,80] we performed additional tests to confirm that the protective effect of PPHA on RNA was detectable by RT-qPCR as well, which allowed both lower dsRNA concentrations (1 mg/L) and lower RNase I activities (0.002−0.2 U) to be used (Figure 4A). Concentrations of dsRNA decreased when exposed to increasing RNase I activities, but the inclusion of PPHA increased remaining dsRNA concentrations by almost one to two orders of magnitude (Figure 4A). An additional experiment using 0.008 U RNase I demonstrated consistent suppression of enzymatic degradation of dsRNA by PPHA at different time


https://doi.org/10.1021/acs.est.3c05019
Environ. Sci. Technol. 2023, 57, 16086−16096

points up to 1.5 h (Figure S14). Consequently, the suppression of enzymatic degradation by HAs also affects measurements of RNA concentrations by application-relevant approaches like RT-qPCR.

**4. Inhibition of RNase I-Mediated RNA Degradation in Environmental Systems.** We subsequently examined whether DOM in environmental samples, specifically in river water and soil extract, could also protect dsRNA against enzymatic degradation, as observed previously with the DOM isolates. To assess the extent of enzymatic degradation suppression by environmental DOM, the hydrolysis product concentrations were compared between a pH-matched buffer control and the natural samples. To exclude dsRNA degradation mediated by naturally occurring extracellular RNases, we additionally measured the concentration of the hydrolysis product in the natural samples without the addition of RNase I.

Over a period of 16.7 h, we did not observe 3-AMP generation in the river water control, but we found that the buffer control had a 3′-AMP generation of 6.0(±0.5) $\mu$M upon the inclusion of RNase I over the same duration (Figure 4B). In contrast, when RNase I was applied to the river water, we found that the 3′-AMP generation was reduced compared to the buffer control, corresponding to an inhibition extent of 38.5(±0.1)% ($p$ = 0.045). Due to the presence of DOM at a concentration of 2.4 $mg_C$/L in the river water sample as well as the consistent pH and temperature between the buffer control and sample, our result suggests that DOM present in the river water protected dsRNA against enzymatic degradation.

We applied an organic MOPS buffer instead of an inorganic buffer species during the preparation of the soil extract in order to prevent competition for binding sites with RNA (Section S3.1).[16] However, the carbon contributed by MOPS masked the contribution of extracted DOM to the organic carbon content. Therefore, we estimated the extracted DOM concentration using light absorbance, which we assumed to predominantly result from DOM. We divided the measured UV−vis absorbance at 254 nm (0.70 ± 0.01 $cm^{-1}$, Table S4) by the specific ultraviolet absorbance ($SUVA_{254\ nm}$) of ESFA (4.6 L $mg_C^{-1}m^{-1}$).[81] This calculation yielded an estimated DOM concentration of 15.2(± 0.2) $mg_C$/L, which when diluted with reactants resulted in a final DOM concentration of 11.4(± 0.2) $mg_C$/L.

Similar to our observation with the river water control, dsRNA degradation was not detected in the soil extract control (Figure 4C), suggesting that extracellular RNases in the soil extract did not contribute to dsRNA degradation within 7 h. In contrast, the buffer control containing RNase I had a 3′-AMP generation of 11.6(±0.4) $\mu$M. The soil extract suppressed RNase I-mediated degradation of dsRNA, as evidenced by the reduction of the 3′-AMP concentration by 45.88(±0.02)% relative to the control ($p$ = 0.005). This result suggested that DOM present in the soil extract contributed to the protection of RNA from enzymatic degradation.

**5. Environmental Implications.** To evaluate the site-independent binding of DOM to RNA in aqueous solutions, we adapted EMSA, a well-established method for evaluating RNA-protein binding.[50,51] In conventional EMSA, the differential migration of the free and bound RNA within the gel is utilized to determine binding. However, the use of a gel running buffer with a fixed solution chemistry in EMSA limits the determination of the effect of solution chemistry on binding.[50,51] Unlike the traditional EMSA, our adapted gel electrophoresis technique detected binding by measuring the suppression of fluorescence due to the reduced intercalation of dye into RNA bound by homopeptides or DOM. As a result, gel electrophoresis distinguished RNA that is bound at all sites by DOM from RNA that is unbound or partially bound.

Using gel electrophoresis, we revealed that the binding of DOM to RNA remained unaffected by tested RNA properties (i.e., length or type). Future studies could examine the binding of DOM to other RNA molecules (e.g., ribosomal RNA and transfer RNA). In contrast, the DOM properties (i.e., DOM type) played a key role in binding. HAs consistently bound to RNA, whereas FAs and NOM did not. The OM type has also been shown to be a key factor determining binding of OM to other biomolecules such as proteins.[58,60] The higher RNA binding capacity of HAs was correlated to their intrinsic properties, such as lower polarity and carboxyl charge density, which led us to hypothesize that binding may be driven by the hydrophobic effect and reduced electrostatic repulsion.

Although RNase I-mediated RNA degradation exceeded rates observed in environmental systems,[22,61] the protective effect of HA remained consistent across varying RNase I activities. At 8−10 $mg_C$/L, within the upper limit of environmentally reported DOM concentrations,[76−78] HAs inhibited nuclease-mediated degradation of RNA to a higher extent than FAs. The higher suppression by HAs may result from their enhanced capacity to bind RNA, which reduces the ability of RNase I to access RNA. An additional consideration maybe the enhanced encapsulation of nucleases by HAs relative to FAs, which may lower their enzymatic activity.[60] Thus, our results suggest that chemically or physically treated microcosms may have different kinetics for RNA degradation in comparison to natural systems if the treatment alters DOM properties such that its binding to RNA is impacted.

The increased persistence of RNA in the presence of DOM has broad environmental implications, specifically in the context of emerging applications of RNA. For example, the suppression of mineral-catalyzed hydrolysis of RNA by DOM could increase the persistence of dsRNA biopesticides in relevant soils and sediments.[17] The increased persistence of dsRNA biopesticides may increase risks posed to nontarget organisms,[15] particularly if bioactivity of dsRNA is retained upon binding by DOM. Our findings additionally suggest that the protective effect of DOM in wastewater[82,83] needs to be considered when modeling degradation rates of free genomic viral RNA[84] in the context of wastewater-based epidemiology. Similarly, DOM may be considered when modeling RNA degradation rates in ecological surveys. Thus, improved estimations of RNA persistence in environmental systems containing DOM will aid the successful deployment of emerging RNA technologies.

## ■ ASSOCIATED CONTENT

### Supporting Information

The Supporting Information is available free of charge at https://pubs.acs.org/doi/10.1021/acs.est.3c05019.

Materials and supplies, RNA and DOM characteristics, characterization of natural soil and river samples, homopeptides characteristics, gel electrophoresis, HPLC protocol, RT-qPCR assay, and supplementary results (PDF)



https://doi.org/10.1021/acs.est.3c05019
Environ. Sci. Technol. 2023, 57, 16086−16096

## AUTHOR INFORMATION


### Corresponding Author

**Kimberly M. Parker** − *Department of Energy, Environmental & Chemical Engineering, Washington University in St. Louis, Missouri 63130, United States;* orcid.org/0000-0002-5380-8893; Phone: (314) 935-3461; Email: kmparker@wustl.edu

### Authors

**Anamika Chatterjee** − *Department of Energy, Environmental & Chemical Engineering, Washington University in St. Louis, Missouri 63130, United States*

**Ke Zhang** − *Department of Energy, Environmental & Chemical Engineering, Washington University in St. Louis, Missouri 63130, United States;* Present Address: Department of Civil and Environmental Engineering, University of Michigan, Ann Arbor, Michigan 48109, United States; orcid.org/0000-0001-6407-8016

Complete contact information is available at: https://pubs.acs.org/10.1021/acs.est.3c05019


### Notes

The authors declare no competing financial interest.

## ACKNOWLEDGMENTS

This work is supported by the Biotechnology Risk Assessment Grant Program Award 2017-33522-26998 from the U.S. Department of Agriculture (K.M.P., A.C., and K.Z.), ACS − Petroleum Research Fund 60057-DNI4 (K.M.P. and A.C.), and N.S.F. CAREER Award 2046602 (K.M.P.). We thank Fuzhong Zhang and Jacqueline Rogers (Department of Energy, Environmental and Chemical Engineering, Washington University in St. Louis) for access to the gel imaging system and water characterization measurements, respectively. We also acknowledge the Chemical and Environmental Analysis Facility (CEAF) at Washington University in St. Louis for access to the TOC analyzer.

## REFERENCES


(1) Torti, A.; Lever, M. A.; Jørgensen, B. B. Origin, Dynamics, and Implications of Extracellular DNA Pools in Marine Sediments. *Mar. Genomics* **2015**, *24*, 185−196.

(2) Carini, P.; Marsden, P. J.; Leff, J. W.; Morgan, E. E.; Strickland, M. S.; Fierer, N. Relic DNA Is Abundant in Soil and Obscures Estimates of Soil Microbial Diversity. *Nat. Microbiol.* **2016**, *2* (3), 1−6.

(3) Mauvisseau, Q.; Harper, L. R.; Sander, M.; Hanner, R. H.; Kleyer, H.; Deiner, K. The Multiple States of Environmental DNA and What Is Known about Their Persistence in Aquatic Environments. *Environ. Sci. Technol.* **2022**, *56* (9), 5322−5333.

(4) Mao, D.; Luo, Y.; Mathieu, J.; Wang, Q.; Feng, L.; Mu, Q.; Feng, C.; Alvarez, P. J. J. Persistence of Extracellular DNA in River Sediment Facilitates Antibiotic Resistance Gene Propagation. *Environ. Sci. Technol.* **2014**, *48* (1), 71−78.

(5) Yates, M. C.; Derry, A. M.; Cristescu, M. E. Environmental RNA: A Revolution in Ecological Resolution? *Trends Ecol. Evol.* **2021**, *36* (7), 601−609.

(6) Cristescu, M. E. Can Environmental RNA Revolutionize Biodiversity Science? *Trends Ecol. Evol.* **2019**, *34* (8), 694−697.

(7) Peccia, J.; Zulli, A.; Brackney, D. E.; Grubaugh, N. D.; Kaplan, E. H.; Casanovas-Massana, A.; Ko, A. I.; Malik, A. A.; Wang, D.; Wang, M.; Warren, J. L.; Weinberger, D. M.; Arnold, W.; Omer, S. B. Measurement of SARS-CoV-2 RNA in Wastewater Tracks Community Infection Dynamics. *Nat. Biotechnol.* **2020**, *38* (10), 1164−1167.

(8) Ahmed, W.; Angel, N.; Edson, J.; Bibby, K.; Bivins, A.; O'Brien, J. W.; Choi, P. M.; Kitajima, M.; Simpson, S. L.; Li, J.; Tscharke, B.; Verhagen, R.; Smith, W. J. M.; Zaugg, J.; Dierens, L.; Hugenholtz, P.; Thomas, K. V.; Mueller, J. F. First Confirmed Detection of SARS-CoV-2 in Untreated Wastewater in Australia: A Proof of Concept for the Wastewater Surveillance of COVID-19 in the Community. *Sci. Total Environ.* **2020**, *728*, 138764.

(9) Silverman, A. I.; Boehm, A. B. Systematic Review and Meta-Analysis of the Persistence and Disinfection of Human Coronaviruses and Their Viral Surrogates in Water and Wastewater. *Environ. Sci. Technol. Lett.* **2020**, *7* (8), 544−553.

(10) Gordon, K. H. J.; Waterhouse, P. M. RNAi for Insect-Proof Plants. *Nat. Biotechnol.* **2007**, *25* (11), 1231−1232.

(11) Fletcher, S. J.; Reeves, P. T.; Hoang, B. T.; Mitter, N. A Perspective on RNAi-Based Biopesticides. *Front. Plant Sci.* **2020**, *11*, 51.

(12) Cagliari, D.; Dias, N. P.; Galdeano, D. M.; dos Santos, E. Á.; Smagghe, G.; Zotti, M. J. Management of Pest Insects and Plant Diseases by Non-Transformative RNAi. *Front. Plant Sci.* **2019**, *10*, 1319.

(13) San Miguel, K.; Scott, J. G. The next Generation of Insecticides: dsRNA Is Stable as a Foliar-Applied Insecticide. *Pest Manag. Sci.* **2016**, *72* (4), 801−809.

(14) Parker, K. M.; Sander, M. Environmental Fate of Insecticidal Plant-Incorporated Protectants from Genetically Modified Crops: Knowledge Gaps and Research Opportunities. *Environ. Sci. Technol.* **2017**, *51* (21), 12049−12057.

(15) Lundgren, J. G.; Duan, J. J. RNAi-Based Insecticidal Crops: Potential Effects on Nontarget Species. *BioScience* **2013**, *63* (8), 657−665.

(16) Sodnikar, K.; Parker, K.; Stump, S.; ThomasArrigo, L. K.; Sander, M. Adsorption of Double-Stranded Ribonucleic Acids (dsRNA) to Iron (Oxyhydr-)Oxides Surfaces: Comparative Analysis of Model dsRNA Molecules and Deoxyribonucleic Acids (DNA). *Environ. Sci. Process. Impacts* **2021**, *23*, 605.

(17) Zhang, K.; Ho, K.-P.; Chatterjee, A.; Park, G.; Li, Z.; Catalano, J. G.; Parker, K. M. RNA Hydrolysis at Mineral-Water Interfaces. *Environ. Sci. Technol.* **2023**, *57* (22), 8280−8288.

(18) Blum, S. A. E.; Lorenz, M. G.; Wackernagel, W. Mechanism of Retarded DNA Degradation and Prokaryotic Origin of DNases in Nonsterile Soils. *Syst. Appl. Microbiol.* **1997**, *20* (4), 513−521.

(19) Romanowski, G.; Lorenz, M. G.; Sayler, G.; Wackernagel, W. Persistence of Free Plasmid DNA in Soil Monitored by Various Methods, Including a Transformation Assay. *Appl. Environ. Microbiol.* **1992**, *58* (9), 3012−3019.

(20) Nielsen, K. M.; Johnsen, P. J.; Bensasson, D.; Daffonchio, D. Release and Persistence of Extracellular DNA in the Environment. *Environ. Biosafety Res.* **2007**, *6* (1−2), 37−53.

(21) Ahmed, W.; Bertsch, P. M.; Bibby, K.; Haramoto, E.; Hewitt, J.; Huygens, F.; Gyawali, P.; Korajkic, A.; Riddell, S.; Sherchan, S. P.; Simpson, S. L.; Sirikanchana, K.; Symonds, E. M.; Verhagen, R.; Vasan, S. S.; Kitajima, M.; Bivins, A. Decay of SARS-CoV-2 and Surrogate Murine Hepatitis Virus RNA in Untreated Wastewater to Inform Application in Wastewater-Based Epidemiology. *Environ. Res.* **2020**, *191*, 110092.

(22) Albright, V. C.; Wong, C. R.; Hellmich, R. L.; Coats, J. R. Dissipation of Double-Stranded RNA in Aquatic Microcosms. *Environ. Toxicol. Chem.* **2017**, *36* (5), 1249−1253.

(23) Parker, K. M.; Barragán Borrero, V.; van Leeuwen, D. M.; Lever, M. A.; Mateescu, B.; Sander, M. Environmental Fate of RNA Interference Pesticides: Adsorption and Degradation of Double-Stranded RNA Molecules in Agricultural Soils. *Environ. Sci. Technol.* **2019**, *53* (6), 3027−3036.

(24) Decrey, L.; Kazama, S.; Udert, K. M.; Kohn, T. Ammonia as an In Situ Sanitizer: Inactivation Kinetics and Mechanisms of the ssRNA Virus MS2 by $NH_3$. *Environ. Sci. Technol.* **2015**, *49* (2), 1060−1067.

(25) Zhang, K.; Hodge, J.; Chatterjee, A.; Moon, T. S.; Parker, K. M. Duplex Structure of Double-Stranded RNA Provides Stability against

Hydrolysis Relative to Single-Stranded RNA. *Environ. Sci. Technol.* **2021**, *55*, 8045−8053.
(26) Chatterjee, A.; Zhang, K.; Rao, Y.; Sharma, N.; Giammar, D. E.; Parker, K. M. Metal-Catalyzed Hydrolysis of RNA in Aqueous Environments. *Environ. Sci. Technol.* **2022**, *56*, 3564−3574.
(27) Green, M. R.; Sambrook, J. How to Win the Battle with RNase. *Cold Spring Harb. Protoc.* **2019**, *2019* (2), pdb.top101857.
(28) Miyamoto, T.; Okano, S.; Kasai, N. Irreversible Thermoinactivation of Ribonuclease-A by Soft-Hydrothermal Processing. *Biotechnol. Prog.* **2009**, *25* (6), 1678−1685.
(29) Cai, P.; Huang, Q.-Y.; Zhang, X.-W. Interactions of DNA with Clay Minerals and Soil Colloidal Particles and Protection against Degradation by DNase. *Environ. Sci. Technol.* **2006**, *40* (9), 2971−2976.
(30) Demanèche, S.; Jocteur-Monrozier, L.; Quiquampoix, H.; Simonet, P. Evaluation of Biological and Physical Protection against Nuclease Degradation of Clay-Bound Plasmid DNA. *Appl. Environ. Microbiol.* **2001**, *67*, 293.
(31) Pietramellara, G.; Ascher, J.; Borgogni, F.; Ceccherini, M. T.; Guerri, G.; Nannipieri, P. Extracellular DNA in Soil and Sediment: Fate and Ecological Relevance. *Biol. Fertil. Soils* **2009**, *45* (3), 219−235.
(32) Cai, P.; Huang, Q.; Chen, W.; Zhang, D.; Wang, K.; Jiang, D.; Liang, W. Soil Colloids-Bound Plasmid DNA: Effect on Transformation of E. Coli and Resistance to DNase I Degradation. *Soil Biol. Biochem.* **2007**, *39* (5), 1007−1013.
(33) Romanowski, G.; Lorenz, M. G.; Wackernagel, W. Adsorption of Plasmid DNA to Mineral Surfaces and Protection against DNase I. *Appl. Environ. Microbiol.* **1991**, *57* (4), 1057−1061.
(34) Paget, E.; Monrozier, L. J.; Simonet, P. Adsorption of DNA on Clay Minerals: Protection against DNase I and Influence on Gene Transfer. *FEMS Microbiol. Lett.* **1992**, *97* (1−2), 31−39.
(35) Khanna, M.; Stotzky, G. Transformation of *Bacillus Subtilis* by DNA Bound on Montmorillonite and Effect of DNase on the Transforming Ability of Bound DNA. *Appl. Environ. Microbiol.* **1992**, *58* (6), 1930−1939.
(36) Lorenz, M. G.; Wackernagel, W. Bacterial Gene Transfer by Natural Genetic Transformation in the Environment. *Microbiol. Rev.* **1994**, *58* (3), 563−602.
(37) Mitter, N.; Worrall, E. A.; Robinson, K. E.; Li, P.; Jain, R. G.; Taochy, C.; Fletcher, S. J.; Carroll, B. J.; Lu, G. Q. M.; Xu, Z. P. Clay Nanosheets for Topical Delivery of RNAi for Sustained Protection against Plant Viruses. *Nat. Plants* **2017**, *3*, 16207.
(38) Franchi, M.; Gallori, E. A Surface-Mediated Origin of the RNA World: Biogenic Activities of Clay-Adsorbed RNA Molecules. *Gene* **2005**, *346*, 205−214.
(39) Crecchio, C.; Ruggiero, P.; Curci, M.; Colombo, C.; Palumbo, G.; Stotzky, G. Binding of DNA from Bacillus Subtilis on Montmorillonite-Humic Acids-Aluminum or Iron Hydroxypolymers. *Soil Sci. Soc. Am. J.* **2005**, *69* (3), 834−841.
(40) Chowdhury, N. N.; Wiesner, M. R. Persistence and Environmental Relevance of Extracellular Antibiotic Resistance Genes: Regulation by Nanoparticle Association. *Environ. Eng. Sci.* **2021**, *38* (12), 1129−1139.
(41) Stotzky, G. Persistence and Biological Activity in Soil of the Insecticidal Proteins from Bacillus Thuringiensis, Especially from Transgenic Plants. *Plant Soil* **2005**, *266* (1−2), 77−89.
(42) Pietramellara, G.; Ascher, J.; Borgogni, F.; Ceccherini, M. T.; Guerri, G.; Nannipieri, P. Extracellular DNA in Soil and Sediment: Fate and Ecological Relevance. *Biol. Fertil. Soils* **2009**, *45* (3), 219−235.
(43) Chowdhury, N. N.; Cox, A. R.; Wiesner, M. R. Nanoparticles as Vectors for Antibiotic Resistance: The Association of Silica Nanoparticles with Environmentally Relevant Extracellular Antibiotic Resistance Genes. *Sci. Total Environ.* **2021**, *761*, 143261.
(44) Nguyen, T. H.; Elimelech, M. Adsorption of Plasmid DNA to a Natural Organic Matter-Coated Silica Surface: Kinetics, Conformation, and Reversibility. *Langmuir* **2007**, *23* (6), 3273−3279.
(45) Nguyen, T. H.; Chen, K. L. Role of Divalent Cations in Plasmid DNA Adsorption to Natural Organic Matter-Coated Silica Surface. *Environ. Sci. Technol.* **2007**, *41* (15), 5370−5375.
(46) Lu, N.; Zilles, J. L.; Nguyen, T. H. Adsorption of Extracellular Chromosomal DNA and Its Effects on Natural Transformation of Azotobacter Vinelandii. *Appl. Environ. Microbiol.* **2010**, *76* (13), 4179−4184.
(47) Lu, N.; Mylon, S. E.; Kong, R.; Bhargava, R.; Zilles, J. L.; Nguyen, T. H. Interactions between Dissolved Natural Organic Matter and Adsorbed DNA and Their Effect on Natural Transformation of *Azotobacter Vinelandii*. *Sci. Total Environ.* **2012**, *426*, 430−435.
(48) Crecchio, C.; Stotzky, G. Binding of DNA on Humic Acids: Effect on Transformation of Bacillus Subtilis and Resistance to DNase. *Soil Biol. Biochem.* **1998**, *30* (8−9), 1061−1067.
(49) Saeki, K.; Ihyo, Y.; Sakai, M.; Kunito, T. Strong Adsorption of DNA Molecules on Humic Acids. *Environ. Chem. Lett.* **2011**, *9* (4), 505−509.
(50) Ryder, S. P.; Recht, M. I.; Williamson, J. R. Quantitative Analysis of Protein-RNA Interactions by Gel Mobility Shift. In *RNA-Protein Interaction Protocols*; Lin, R.-J., Ed.; Methods in Molecular Biology; Humana Press: Totowa, NJ, 2008; pp 99−115 DOI: 10.1007/978-1-60327-475-3_7.
(51) Seo, M.; Lei, L.; Egli, M. Label-Free Electrophoretic Mobility Shift Assay (EMSA) for Measuring Dissociation Constants of Protein-RNA Complexes. *Curr. Protoc. Nucleic Acid Chem.* **2019**, *76* (1), No. e70.
(52) Mann, A.; Richa, R.; Ganguli, M. DNA Condensation by Poly-l-Lysine at the Single Molecule Level: Role of DNA Concentration and Polymer Length. *J. Controlled Release* **2008**, *125* (3), 252−262.
(53) Baum, J. A.; Roberts, J. K. Chapter Five - Progress Towards RNAi-Mediated Insect Pest Management. In *Advances in Insect Physiology*; Dhadialla, T. S., Gill, S. S., Eds.; Insect Midgut and Insecticidal Proteins; Academic Press: 2014; Vol. *47*, pp 249−295 DOI: 10.1016/B978-0-12-800197-4.00005-1.
(54) Das, P. R.; Sherif, S. M. Application of Exogenous dsRNAs-Induced RNAi in Agriculture: Challenges and Triumphs. *Front. Plant Sci.* **2020**, *11*, 946.
(55) Gruber, A. R.; Lorenz, R.; Bernhart, S. H.; Neuböck, R.; Hofacker, I. L. The Vienna RNA Websuite. *Nucleic Acids Res.* **2008**, *36*, W70−W74.
(56) Nwokeoji, A. O.; Kilby, P. M.; Portwood, D. E.; Dickman, M. J. Accurate Quantification of Nucleic Acids Using Hypochromicity Measurements in Conjunction with UV Spectrophotometry. *Anal. Chem.* **2017**, *89* (24), 13567−13574.
(57) *RNase I (10 U/μL)*. https://www.thermofisher.com/order/catalog/product/EN0601 (accessed 2022-09-08).
(58) Tomaszewski, J. E.; Madliger, M.; Pedersen, J. A.; Schwarzenbach, R. P.; Sander, M. Adsorption of Insecticidal Cry1Ab Protein to Humic Substances. 2. Influence of Humic and Fulvic Acid Charge and Polarity Characteristics. *Environ. Sci. Technol.* **2012**, *46* (18), 9932−9940.
(59) Sander, M.; Tomaszewski, J. E.; Madliger, M.; Schwarzenbach, R. P. Adsorption of Insecticidal Cry1Ab Protein to Humic Substances. 1. Experimental Approach and Mechanistic Aspects. *Environ. Sci. Technol.* **2012**, *46*, 9923.
(60) Tomaszewski, J. E.; Schwarzenbach, R. P.; Sander, M. Protein Encapsulation by Humic Substances. *Environ. Sci. Technol.* **2011**, *45* (14), 6003−6010.
(61) Zhang, K.; Wei, J.; Huff Hartz, K. E.; Lydy, M. J.; Moon, T. S.; Sander, M.; Parker, K. M. Analysis of RNA Interference (RNAi) Biopesticides: Double-Stranded RNA (dsRNA) Extraction from Agricultural Soils and Quantification by RT-qPCR. *Environ. Sci. Technol.* **2020**, *54* (8), 4893−4902.
(62) Xiangbi Chen, X. Z.; Yajun Hu, C. L.; Yirong Su, J. W. Influence of Extractants and Filter Materials in the Extraction of Dissolved Organic Matter (DOM) from Subtropical Agricultural Soil. *Emir. J. Food Agric.* **2018**, 165.

(63) Li, R.; Xi, B.; Tan, W.; Yuan, Y. Spatiotemporal Heterogeneous Effects of Microplastics Input on Soil Dissolved Organic Matter (DOM) under Field Conditions. *Sci. Total Environ.* **2022**, *847*, 157605.
(64) Bysell, H.; Malmsten, M. Interactions between Homopolypeptides and Lightly Cross-Linked Microgels. *Langmuir* **2009**, *25* (1), 522−528.
(65) Shinozuka, T.; Shibata, M.; Yamaguchi, T. Molecular Weight Characterization of Humic Substances by MALDI-TOF-MS. *J. Mass Spectrom. Soc. Jpn.* **2004**, *52* (1), 29−32.
(66) Chin, Y.-P.; Aiken, G.; O'Loughlin, E. Molecular Weight, Polydispersity, and Spectroscopic Properties of Aquatic Humic Substances. *Environ. Sci. Technol.* **1994**, *28* (11), 1853−1858.
(67) *TAE Buffer (Tris-acetate-EDTA) (50X)*. https://www.thermofisher.com/order/catalog/product/B49 (accessed 2022-12-07).
(68) *GraphPad Prism 9 Curve Fitting Guide - Equation: Specific binding with Hill slope*. https://www.graphpad.com/guides/prism/latest/curve-fitting/reg_specific_hill.htm (accessed 2022-09-07).
(69) Bechhofer, D. H.; Deutscher, M. P. Bacterial Ribonucleases and Their Roles in RNA Metabolism. *Crit. Rev. Biochem. Mol. Biol.* **2019**, *54* (3), 242−300.
(70) Luhtala, N.; Parker, R. T2 Family Ribonucleases: Ancient Enzymes with Diverse Roles. *Trends Biochem. Sci.* **2010**, *35* (5), 253−259.
(71) Shen, V.; Schlessinger, D. RNase I of Escherichia Coli. In *The Enzymes*; Academic Press Inc.: New York, 1982; Vol. *15B*, pp 503−506.
(72) Grünberg, S.; Coxam, B.; Chen, T.-H.; Dai, N.; Saleh, L.; Corrêa, I. R., Jr; Nichols, N. M.; Yigit, E. E. Coli RNase I Exhibits a Strong Ca2+-Dependent Inherent Double-Stranded RNase Activity. *Nucleic Acids Res.* **2021**, *49* (9), 5265−5277.
(73) *Nucleases (DNases and RNases)*. https://www.sigmaaldrich.com/US/en/products/protein-biology/proteins-and-enzymes/nucleases (accessed 2022-08-11).
(74) Sherbet, G. V.; Lakshmi, M. S.; Cajone, F. Isoelectric Characteristics and the Secondary Structure of Some Nucleic Acids. *Biophys. Struct. Mech.* **1983**, *10* (3), 121−128.
(75) Lichtenberg, S. S.; Laisney, J.; Elhaj Baddar, Z.; Tsyusko, O. V.; Palli, S. R.; Levard, C.; Masion, A.; Unrine, J. M. Comparison of Nanomaterials for Delivery of Double-Stranded RNA in *Caenorhabditis Elegans*. *J. Agric. Food Chem.* **2020**, *68* (30), 7926−7934.
(76) Thurman, E. M. *Organic Geochemistry of Natural Waters*; Springer Netherlands: Dordrecht, 1985; DOI: 10.1007/978-94-009-5095-5.
(77) Moeller, J. R.; Minshall, G. W.; Cummins, K. W.; Petersen, R. C.; Cushing, C. E.; Sedell, J. R.; Larson, R. A.; Vannote, R. L. Transport of Dissolved Organic Carbon in Streams of Differing Physiographic Characteristics. *Org. Geochem.* **1979**, *1* (3), 139−150.
(78) Spencer, R. G. M.; Butler, K. D.; Aiken, G. R. Dissolved Organic Carbon and Chromophoric Dissolved Organic Matter Properties of Rivers in the USA. *J. Geophys. Res. Biogeosciences* **2012**, *117* (G3), G03001.
(79) Dugas, H.; Penney, C. Bioorganic Chemistry of the Phosphates. In *Bioorganic Chemistry: A Chemical Approach to Enzyme Action*; Springer US: 1981; pp 93−178.
(80) Marshall, N. T.; Vanderploeg, H. A.; Chaganti, S. R. Environmental (e)RNA Advances the Reliability of eDNA by Predicting Its Age. *Sci. Rep.* **2021**, *11* (1), 2769.
(81) Kwon, D.; Sovers, M. J.; Grassian, V. H.; Kleiber, P. D.; Young, M. A. Optical Properties of Humic Material Standards: Solution Phase and Aerosol Measurements. *ACS Earth Space Chem.* **2018**, *2* (11), 1102−1111.
(82) Xiao, K.; Abbt-Braun, G.; Horn, H. Changes in the Characteristics of Dissolved Organic Matter during Sludge Treatment: A Critical Review. *Water Res.* **2020**, *187*, 116441.
(83) Shi, W.; Zhuang, W.-E.; Hur, J.; Yang, L. Monitoring Dissolved Organic Matter in Wastewater and Drinking Water Treatments Using Spectroscopic Analysis and Ultra-High Resolution Mass Spectrometry. *Water Res.* **2021**, *188*, 116406.
(84) Wurtzer, S.; Waldman, P.; Ferrier-Rembert, A.; Frenois-Veyrat, G.; Mouchel, J. M.; Boni, M.; Maday, Y.; Marechal, V.; Moulin, L. Several Forms of SARS-CoV-2 RNA Can Be Detected in Wastewaters: Implication for Wastewater-Based Epidemiology and Risk Assessment. *Water Res.* **2021**, *198*, 117183.